



Reducing carbon footprint in high H₂S emissions: A synergistic microalgal-bacterial solution for sugarcane biorefineries

André do Vale Borges^{a,b}, Andrés Felipe Torres Franco^b,
Márcia Helena Rissato Zamariolli Damianovic^b, Raúl Muñoz Torre^{a,c,*}

^a Institute of Sustainable Processes, Dr. Mergelina, s/n, Valladolid 47011, Spain

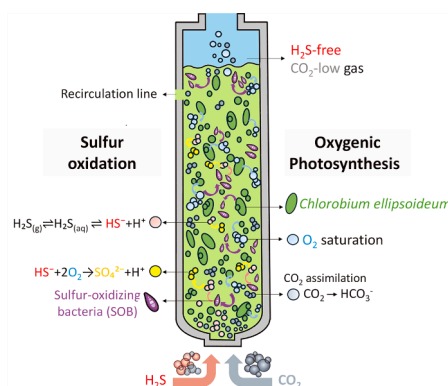
^b Biological Processes Laboratory (LPB), São Carlos School of Engineering (EESC), University of São Paulo (USP), Av. João Dagnone, 1100, Santa Angelina, São Carlos, São Paulo 13563-120, Brazil

^c Department of Chemical Engineering and Environmental Technology, School of Industrial Engineering, University of Valladolid, Dr. Mergelina, s/n, Valladolid 47011, Spain

HIGHLIGHTS

- Extreme H₂S emissions (up to 72 gS-H₂S m⁻³) were fully abated at all off-gas flows.
- Alkalinity (1.8 – 3.4 g L⁻¹) sustained 98.2 % CO₂ biofixation by *Chloroidium* sp.
- Microbial adaptation to high H₂S boosted biomass growth, enhancing sulfur oxidation.
- Five folds lower nitrate inputs than conventional CMB systems for biogas treatment.
- Biodigested vinasse is a promising pH stabilizer for cost-effective gas treatment.

GRAPHICAL ABSTRACT



ARTICLE INFO

Keywords:

Biogas upgrading
Vinasse circular bioeconomy
CO₂ sequestration
Hydrogen sulfide removal
Microalgal-bacterial system

ABSTRACT

Sugarcane vinasse, a major by-product of ethanol production, poses environmental and health risks due to its high sulfate content, promoting severe hydrogen sulfide (H₂S) formation (up to 50,000 ppm_v) during acidogenic fermentation. The resulting H₂S and high carbon dioxide (CO₂) levels in off-gas create serious hazards, often leading to conventional desulfurization systems' clogging and high maintenance. This study is the first to investigate a *Chloroidium*-based combined microalgal-bacterial (CMB) system for simultaneous, high-strength H₂S abatement and CO₂ sequestration from these challenging vinasse fermentation off-gas streams. Utilizing a 14 L bubble column photobioreactor under increasing gas flow conditions, the system achieved 100 % H₂S and 98.2 % CO₂ removal efficiencies within 72 h, with a maximum H₂S elimination capacity of 30.3 gS-H₂S m⁻³ h⁻¹. A comprehensive sulfur mass balance revealed that up to 99 % of theoretical sulfate was consumed by the consortium for biomass growth, demonstrating efficient sulfur valorization. Performance was sustained by elevated dissolved oxygen (averaging 15.0 g L⁻¹), ensuring complete H₂S oxidation to sulfate without inhibitory

* Corresponding author at: Institute of Sustainable Processes, Dr. Mergelina, s/n, Valladolid 47011, Spain.

E-mail addresses: andreborges@usp.br (A. do Vale Borges), mdamianovic@sc.usp.br (M.H.R. Zamariolli Damianovic), mutora@iq.uva.es (R.M. Torre).

<https://doi.org/10.1016/j.jhazmat.2025.139539>

Received 22 April 2025; Received in revised form 18 July 2025; Accepted 10 August 2025

Available online 12 August 2025

0304-3894/© 2025 The Author(s). Published by Elsevier B.V. This is an open access article under the CC BY license (<http://creativecommons.org/licenses/by/4.0/>).

intermediate accumulation or clogging. The system's robustness was further supported by *Chloroidium ellipsoideum*'s adaptation to high H_2S loads (up to $72.0 \text{ g-S-H}_2\text{S m}^{-3}$) and optimized inorganic carbon ($1.8\text{--}3.4 \text{ g L}^{-1}$). These results highlight the CMB system's potential as a biologically driven, low-input, clogging-resistant, and highly efficient alternative for acidogenic off-gas treatment and vinasse valorization, offering a scalable and sustainable solution for biorefineries.

1. Introduction

Sugarcane vinasse, the primary by-product of sugar and ethanol production, exhibits significant environmental challenges due to its high organic load, low pH, and elevated mineral content [30]. Although it is widely used as a nutrient-rich fertilizer for sugarcane crops, excessive application can lead to soil salinization, groundwater contamination, nutrient leaching [19,29], and the emission of greenhouse gases (GHGs) such as nitrous oxide [45]. These issues highlight the urgent need for sustainable vinasse management strategies.

Anaerobic digestion (AD) has emerged as a promising solution to address these challenges, offering advantages such as organic matter load reduction, nutrient conservation, and renewable energy generation through biogas production. Conventional single-phase AD systems (1st-AD) have been shown to effectively treat vinasse [21,6]. However, the high sulfate concentrations in vinasse (often exceeding $2.0 \text{ g-SO}_4^{2-} \text{ L}^{-1}$), a result of sulfuric acid addition during ethanol fermentation, promote the growth of sulfate-reducing bacteria (SRB) [14]. This metabolic competition shifts the process towards sulfidogenesis, limiting methane (CH_4) yields and exacerbating the management of sulfur compounds [40]. To mitigate this, recent advancements in high-rate fermentative systems have focused on effectively reducing sulfate from vinasse before methanogenesis. This is achieved by providing optimal conditions, such as maintaining neutral pH and applying appropriate alkali supplementation, which favor SRB activity. Electron donors such as glycerol and lactic acid, produced during juice fermentation, further enhance SRB activity. While thermophilic conditions (55°C) support SRB growth [27, 60,74], they can reduce CH_4 recovery [32], contrasting with mesophilic fermentation (30°C), which enhances acetate accumulation and partial alkalinity, yielding sulfate-free, acetate-enriched vinasse. This approach promises improved methane recovery [10].

Crucially, while these fermentative systems effectively manage sulfate and generate biogas, their off-gas is characterized by exceptionally high concentrations of carbon dioxide (CO_2 , up to 90 %) and hydrogen sulfide (H_2S , up to 5 % or $50,000 \text{ ppm}_v$), which require dedicated and effective treatment. Importantly, hydrogen gas (H_2) is consistently found in undetectable fractions ($<1 \%$) in these off-gases, simplifying subsequent gas management due to its non-flammable nature. Despite the significant potential of novel desulfurization technologies, such as microalgal-bacterial photobioreactors for CO_2 and H_2S abatement, their application under such extreme H_2S emissions from acidogenic sugarcane vinasse treatment reactors has not been tested.

H_2S is a colorless, toxic gas with severe environmental, health, and operational implications, notably in AD systems (Muñoz et al., 2015). Its atmospheric oxidation forms sulfur dioxide (SO_2), contributing to acid rain [66] and biodiversity loss [67]. Additionally, bisulfide ions harm aquatic life [46], and persistent H_2S odors impact human quality of life. In AD systems, H_2S -induced corrosion of pipelines and equipment increases maintenance costs and risks system failures [90]. Moreover, H_2S reduces biogas quality, necessitating desulfurization before utilization [58]. To mitigate these impacts, fermenters must operate as gas-tight systems, routing all gas emissions to appropriate treatment technologies.

Addressing high-strength H_2S and CO_2 emissions in AD is difficult, often involving cost-prohibited alkali supplementation and desulfurization technologies [73]. The effectiveness of these processes is influenced by various operational factors and biogas composition [66]. Among commercially available technologies, physicochemical systems are effective for high H_2S -load streams by enhancing mass transfer [15,

7,92]. In this context, biological desulfurization methods, including phototrophic and chemotrophic approaches, offer several advantages, such as lower operational costs, reduced chemical usage, lower energy demand, and the production of non-hazardous end products [17,44].

Conventional biological gas filtration technologies such as biofilters (BFs), bioscrubbers (BSs), and biotrickling filters (BTFs) are widely applied for biogas desulfurization in AD plants [18,59]. These systems rely on sulfur-oxidizing bacteria (SOB), immobilized on inert packed beds or in suspension in a separate tank, to oxidize H_2S into elemental sulfur or sulfate [58]. Typical removal efficiencies exceed 95 %, with elimination capacities (EC) of up to $160 \text{ g-S-H}_2\text{S m}^{-3} \text{ h}^{-1}$ [9,75,56]. However, they often struggle with elemental sulfur accumulation and oxygen mass transfer limitations, especially under high H_2S loads typical of acidogenic off-gas (up to 5 %).

Photosynthetic biogas upgrading, particularly combined microalgal-bacterial (CMB) systems, is a promising technology for simultaneous H_2S and CO_2 removal. These systems leverage well-established synergy where microalgae provide in-situ oxygen for bacterial oxidation processes, while bacteria detoxify the environment, allowing microalgae to thrive [22,8,81]. Thus, rapid and complete sulfur oxidation to sulfate occurs, preventing elemental sulfur accumulation and associated clogging issues [3,4,68]. This internal oxygen generation also eliminates the need for external oxygen supply. Furthermore, by harnessing the high CO_2 fraction as an inorganic carbon source for microalgal growth, CMB systems reduce bicarbonate supplementation needs and convert a major greenhouse gas into valuable algal biomass [76,77,8], contributing to sustainable development and carbon neutrality [16].

Building on these findings, this study investigates a dual-purpose CMB system for or simultaneous desulfurization of high- H_2S off-gas from mesophilic (30°C) sugarcane vinasse fermentation and CO_2 sequestration to reduce greenhouse gas emissions. An indoor algal pond coupled with an off-gas absorption column was operated across three stages with increasing gas flow rates, maintaining a constant liquid-to-gas (L/G) ratio of 10, and successfully subjected to extreme H_2S loadings of up to $72 \text{ g-S-H}_2\text{S m}^{-3}$. This pioneering approach offers a unique solution to manage high H_2S concentrations in biogas generated by acidogenic systems, specifically tailored to sugarcane biorefineries. By integrating principles of renewable energy and biological valorization, this study not only addresses critical environmental issues like H_2S emissions but also supports broader goals of carbon neutrality, sustainable industrial practices, and fostering a circular bioeconomy.

2. Material and methods

2.1. Experimental apparatus and nutritional aspects

An indoor open algal pond (AP) with a working volume of 14 L (dimensions: $39 \text{ cm} \times 19 \text{ cm} \times 19 \text{ cm}$; surface area: 0.07 m^2) was installed at the Institute of Sustainable Processes (ISP) at the University of Valladolid, Spain. The AP was connected to an external 0.9 L absorption column (AC) via a recirculation line, operating at a controlled room temperature of $27 \pm 1^\circ\text{C}$. This AC unit was operated as a bubble column reactor, devoid of internal packing, where gas-liquid contact facilitated H_2S oxidation and CO_2 dissolution by the suspended microbial community. Liquid recirculation and gas pumping were achieved using two peristaltic pumps (Masterflex 7553–70, Cole Parmer, USA; and Model TDF-SK-Handy pump, Hygiaflex, Spain), respectively.

The system received continuous illumination (24 h light:0 h dark) in

the AP surface at a photosynthetically active radiation (PAR) of $1040 \pm 15 \mu\text{mol m}^{-2} \text{s}^{-1}$ from LED panels (Philips, Spain). The system was consistently fed with a carbon-rich synthetic media via a peristaltic pump (Model TDF-SK-Handy pump, Hygiaflex, Spain). The mineral salt medium (MSM) exhibited the following composition (g L^{-1}): NaHCO_3 , 6; Na_2CO_3 , 3; K_2HPO_4 , 0.94; NaNO_3 , 3.06; NaCl , 2.09; $\text{CaCl}_2 \cdot 2\text{H}_2\text{O}$, 0.02; $\text{FeSO}_4 \cdot 7\text{H}_2\text{O}$, 0.005; $\text{MgSO}_4 \cdot 7\text{H}_2\text{O}$, 0.1. The micronutrient solution added to the medium (5 mL L^{-1}) was composed of (g L^{-1}): $\text{ZnSO}_4 \cdot 7\text{H}_2\text{O}$, 0.1; $\text{MnCl}_4 \cdot 4\text{H}_2\text{O}$, 0.0005; H_3BO_3 , 0.2; $\text{Co}(\text{NO}_3)_2 \cdot 6\text{H}_2\text{O}$, 0.02; $\text{Na}_2\text{MoO}_4 \cdot 2\text{H}_2\text{O}$, 0.02; $\text{CuSO}_4 \cdot 5\text{H}_2\text{O}$, 0.0005; $\text{FeSO}_4 \cdot 7\text{H}_2\text{O}$, 0.07; $\text{EDTA} \cdot 2\text{H}_2\text{O}$, 1.02). To prevent biomass accumulation, two centrifugal submersible pumps (FRCOLOR, China) were installed on opposite sides of the glass structure. The AC consisted of a transparent acrylic bubble column (internal diameter: 3.8 cm; height: 75 cm) fitted with a metal gas diffuser (pore size: $2 \mu\text{m}$) positioned at its base. A schematic diagram of the CMB system is provided in Fig. 1.

2.2. Inoculation and operating conditions

A microalgal cake containing *Chloroidium ellipsoideum* species was collected from a 180 L high-rate algal pond fed with real digestate and a biogas containing 5000 ppm_v of H_2S [36,53]. Fresh aerobic sludge from Valladolid wastewater treatment plant (WWTP) was also used to inoculate the algal-bacterial pond herein used for acidogenic off-gas abatement. The microalgal species were cultivated in MSM with a high carbonate source, as detailed by [54]. The system was initiated with an algal-biomass concentration of 2.0 g-VSS L^{-1} .

The system was subjected to three operational stages (namely I, II, and III), defined by variations in gas flow rates (1.7-, 3.4-, and 6.8 mL min^{-1}) under a constant liquid-to-gas flow rate ratio (L/G) of 10, as reported elsewhere [63]. MSM (Fig. 1, labeled 13) was continuously supplied at 0.74 L d^{-1} while the synthetic biogas mixture (72 % CO_2 , 23 % N_2 , and 5 % H_2S) was introduced into the AC unit (Fig. 1, labeled 1) in a co-current flow with the recirculating liquid phase (Fig. 1, from 8 to 12). As a result, the volume of nutrients supplied per unit volume of gas progressively decreased with increasing gas flow rates, corresponding to 0.30, 0.15, and $0.08 \text{ L MSM per liter of gas}$ in Stages I, II, and III, respectively. This gas simulated the acidogenic off-gas from vinasse fermentation [10] and was obtained by mixing a 22 %/78 % $\text{H}_2\text{S}/\text{N}_2$ synthetic gas mixture with atmospheric air in a mixing chamber

(Fig. 1, labeled 7). Synthetic acidogenic off-gas was used to avoid potential flow rate fluctuations typical of an on-site acidogenic reactor processing raw sugarcane vinasse, which could hinder sulfur oxidation processes due to biomass growth. While the use of this synthetic off-gas ensured controlled and reproducible experimental conditions, it is important to acknowledge that real vinasse-derived biogas typically presents fluctuations and complex impurities that may influence long-term system performance and scalability, representing a limitation that requires consideration for future industrial applications.

Daily liquid phase monitoring comprised the determination of the following parameters: pH, dissolved oxygen (DO), room and AP temperatures (T), and photosynthetic quantum yield (QY). The determination of the concentrations of total organic carbon (TOC), inorganic carbon (IC), total nitrogen (TN), volatile suspended solids (VSS), total dissolved sulfide (TDS), sulfate (SO_4^{2-}), thiosulfate ($\text{S}_2\text{O}_3^{2-}$), nitrite (NO_2^-), and nitrate (NO_3^-), was performed three times a week. Lastly, PAR measurements were conducted weekly. Gas samples for the determination of CO_2 , N_2 , O_2 , and H_2S concentrations were collected daily in duplicate at the inlet and outlet sampling ports of the absorption column (Ports 9 and 10 in Fig. 1). Samples were introduced into a gas chromatograph equipped with a thermal conductivity detector (Model 8890, Agilent Technologies, Santa Clara, CA, USA) via direct injection using a gastight syringe, without the use of any intermediate sampling bags for collection or injection. The sampling lines connecting the ports to the syringe were plastic tubes. While some plastic materials may exhibit H_2S adsorption, the high removal efficiencies (100 % $\text{H}_2\text{S-RE}$) observed and the absence of intermediate sulfur species in the cultivation broth confirm that the reactor's performance was accurately reflected by these measurements, indicating no significant analytical bias from the sampling line material. The GC was equipped with a thermal conductivity detector. For accurate quantification, the instrument was calibrated using certified gas standards (multi-point calibration curves) for all target components prior to experimental campaigns, with regular checks using a mid-range standard. The detection limit for H_2S was typically 100 ppm_v. To ensure methodological reliability, consistent injection volumes and carrier gas flow rates were maintained, and routine instrument maintenance was performed according to manufacturer guidelines.

To ensure the reliability and statistical robustness of our findings, all reported results were derived from a single, continuous experimental

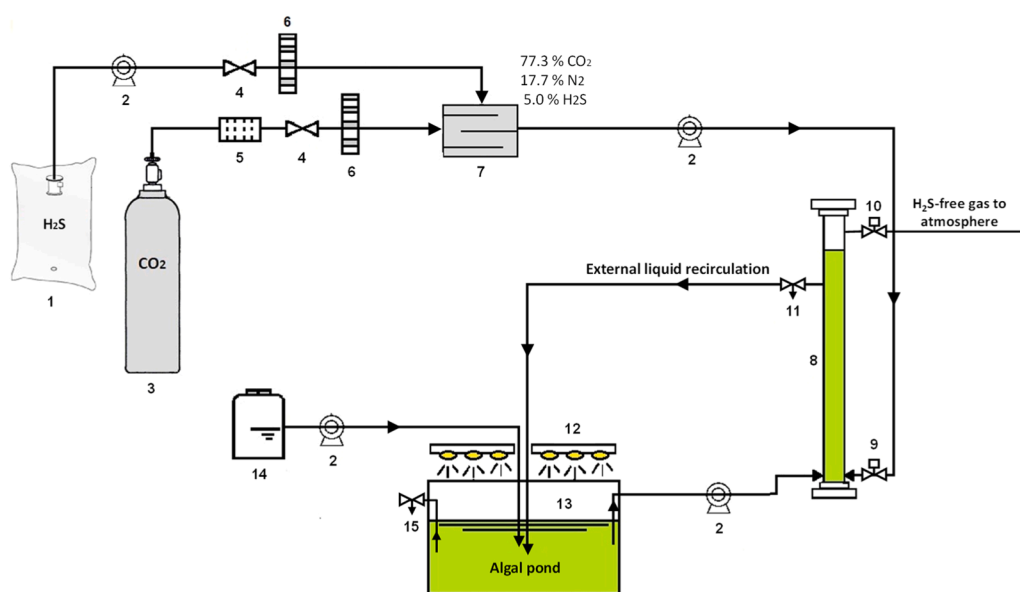


Fig. 1. Sketch of the experimental set-up. (1) 30 L Tedlar bag, (2) peristaltic pumps, (3) CO_2 -cylinder, (4) valves, (5) mass flux controller, (6) rotameters, (7) mixing chamber (8) 0.8 L absorbed column, (9) inlet gas sampling port, (10) outlet gas sampling port, (11) liquid sampling port, (12) LED panels, (13) 14 L algal pond, (14) 2 L nutrient-feeding reservoir, (15) liquid sampling port.

run across three distinct operational stages. Throughout this long-term experiment, all liquid and gas samples were collected and analyzed in duplicate. The numerical results presented represent average values accompanied by their respective standard deviations, calculated from these multiple duplicate measurements over time within each operational stage, thereby confirming the consistency and reliability of the system's performance. Though error bars are not displayed in the figures, this is due to the exceptionally low variability observed in the measurements across the operational stages, with standard deviations frequently being smaller than the data points. This consistent and minimal spread in the data highlights the remarkable stability and robustness of the developed system.

An Eutech Cyberscan pH 510 (Thermo Fisher Scientific Inc., Massachusetts, USA) and an OXI 3310 oximeter (WTW, Germany) were used for pH, temperature and DO determinations in the cultivation broth, respectively. pH was carefully monitored daily at two critical points in the system: the cultivation broth and the outlet of the absorption column (AC), which was sampled via a valve (indicated in Fig. 1). Although no formal pH optimization study was conducted in this work, the operational pH was guided by values reported in prior studies. The system was maintained under alkaline conditions (pH > 9), which are widely recognized to enhance CO₂ and H₂S absorption due to favorable chemical equilibria ([12,25,71]; Markou et al., 2014). The use of carbonated alkaline cultivation media has also been shown to support both efficient biogas upgrading and microalgal viability in long-term operations. QY was measured using a Li-250A light meter (Li-COR Biosciences, Germany). TOC, IC, and TN analysis were conducted in a TOC-VCSH analyzer coupled with a TNM-1 chemiluminescence module (Shimadzu, Japan). The concentrations of NO₂, NO₃, SO₄²⁻, and S₂O₃²⁻ were quantified using HPLC-IC, equipped with a Waters 515 HPLC pump, a conductivity detector (Waters 432), an IC-PAK Anion HC column (4.6 × 150 mm), and an IC-Pak Anion Guard-Pak (Waters). Prior to anion analysis, samples were filtered through membranes with a pore size of 0.22 μm. Sulfide levels were assessed via a highly sensitive photometric method (Merck KGaA, Darmstadt, Germany), allowing for the quantification of HS⁻ and S²⁻ ions within a concentration range of 0.02–1.55 mg L⁻¹. VSS was measured following the Standard Methods for the Examination of Water and Wastewater [5]. Cultivation broth samples were collected after inoculation and at the conclusion of each operating stage, then preserved in 10 % neutral formaldehyde and 5 % Lugol's acid for quantitative assessment of the algal population structure [80]. Gas samples were analyzed using a gas chromatograph (Model 8890, Agilent Technologies, Santa Clara, CA, USA) equipped with a thermal conductivity detector. The temperatures of the detector and injector were kept steady at 170°C and 160°C, respectively, for 5 min. Helium was used as the carrier gas, flowing at a rate of 13.7 mL min⁻¹.

2.3. Performance metrics

The removal efficiencies (REs, %) of H₂S and CO₂ were calculated according to Eq. (1), where Q_{IN} and Q_{OUT} represent the inlet and outlet acidogenic off-gas flow rates (L d⁻¹), respectively, and C_{IN} and C_{OUT} denote the inlet and outlet concentrations (%) of the target pollutants.

$$RE = \frac{(C_{IN} - C_{OUT})}{C_{IN}} \times 100 \quad (1)$$

The H₂S and CO₂ loading rates (LRs) (gS-H₂S m⁻³ h⁻¹ and gC-CO₂ m⁻³ h⁻¹) throughout the operation were calculated using Eq. (2), where Q_{GAS} is the acidogenic off-gas flow rate (m³ d⁻¹), C_{IN, POLLUTANT} is the inlet pollutant (CO₂ and H₂S) concentration (g m⁻³), and V_{COLUMN} is the absorption column volume (m³). C_{IN, POLLUTANT} was calculated using Eq. (3), where %_{POLLUTANT} is the fraction (%) of the pollutant in the gas, MM_{POLLUTANT} is the molar mass of the pollutant and V_{MOLAR} is the molar volume of the pollutant. V_{MOLAR} was calculated according to Eq. (4), where R is the universal gas constant (8.314 J mol⁻¹ K⁻¹ or 0.0821 L atm mol⁻¹ K⁻¹), T is the operating temperature (K), and P

(atm) is the atmospheric pressure. The H₂S and CO₂ elimination capacities (ECs) of the system were calculated using Eq. (5), where LR represents the loading rate (LR) and RE is the removal efficiency. NO₃-REs (%) were calculated using Eq. (6), where N-NO_{3,t} is the total mass (g) of nitrate from the MSM and N-NO_{3,a} is the mass (g) of nitrate accumulated in the pond throughout the operation.

$$LR = \frac{(C_{IN, POLLUTANT} \times Q_{GAS})}{V_{COLUMN}} \quad (2)$$

$$C_{IN, POLLUTANT} = \frac{(\%_{POLLUTANT} \times MM_{POLLUTANT})}{V_{MOLAR}} \quad (3)$$

$$V_{MOLAR} = \frac{(R \times T)}{P} \quad (4)$$

$$EC = (LR \times RE) \quad (5)$$

$$RE = \frac{(N - NO_{3,t} - N - NO_{3,a})}{N - NO_{3,a}} \times 100 \quad (6)$$

2.4. Sulfur mass balance and estimation of consumption

A comprehensive sulfur mass balance was performed for each operational stage to evaluate the fate of sulfur within the system and to estimate its consumption by the microalgal-bacterial consortium. The primary sulfur inputs considered were hydrogen sulfide (H₂S) from the simulated off-gas and magnesium sulfate (MgSO₄·7H₂O) supplied via the mineral salt medium. Key assumptions for this balance included the complete oxidation of all incoming H₂S to soluble sulfate (SO₄²⁻), a premise strongly supported by the observed 100 % H₂S removal efficiencies and the absence of elemental sulfur (S⁰) precipitation. Furthermore, sulfate (SO₄²⁻) was considered the sole significant inorganic sulfur species accumulating in the cultivation broth.

For each operational stage, the following components were quantified:

1. **Total sulfur input from H₂S (S-H₂S,in):** Calculated from the average inlet gas flow rate, inlet H₂S concentration, and stage duration, converting H₂S mass to sulfur mass.
2. **Total sulfur input from MgSO₄·7H₂O (S-MgSO₄,in):** Determined from the average MSM flow rate, MgSO₄·7H₂O concentration in the medium, and stage duration, converting MgSO₄·7H₂O mass to sulfur mass.
3. **Sulfur output as sulfate in effluent (S-SO₄,out):** Since our system had "zero liquid discharge", the "Sulfur Out in Effluent" term was negligible.
4. **Change in sulfate accumulated in reactor liquid (ΔS-reactor):** Calculated from the difference between the final and initial SO₄²⁻ concentrations in the reactor liquid for the stage, multiplied by the reactor working volume, converting SO₄²⁻ mass to sulfur mass.

The **estimated total sulfate consumed by microalgae and bacteria (S-consumed)** (assimilated into biomass) was then determined by the difference between total sulfur inputs and the sum of sulfur outputs and net accumulation:

$$S\text{-consumed} = (S\text{-H}_2\text{S,in} + S\text{-MgSO}_4\text{,in}) - S\text{-SO}_4\text{,out} - \Delta S\text{-reactor}$$

Detailed calculations and raw data are provided in the [Supplementary Material](#).

3. Results and discussion

3.1. Influence of gas flow rate on CO₂ and H₂S abatement

Following inoculation, the rapid synergistic interactions between

SOB and microalgae facilitated an efficient off-gas pollutant removal (CO_2 and H_2S -REs of $95.3 \pm 2.2\%$ and $98.8 \pm 0.9\%$, respectively), within the first three days of operation. During this period, IC concentrations in the cultivation broth reached $1853 \pm 166 \text{ mg IC L}^{-1}$, highlighting the significant contribution of microalgal CO_2 uptake. From day 3 until the end of the operation, CO_2 -RE remained high at $98.2 \pm 0.6\%$, while a complete H_2S removal was sustained, despite increasing gas flow rates (Fig. 2 a). These consistently high removal efficiencies, achieved from the onset, underscore the robustness and rapid acclimation of the algal-bacterial system. Microalgal photosynthesis continuously provided oxygen to support SOB-mediated sulfide oxidation, as further evidenced by the increase in sulfate production across the three operating stages. The sustained vigor of the microalgal biomass growth, coupled with stable quantum yield, and clear patterns of nutrient uptake (sulfate and nitrate assimilation), provide strong indirect evidence of a thriving and highly active microbial population at the core of the observed transformations. Unlike *Chlorella sp.*, which exhibited growth inhibition at H_2S concentrations above 200 ppm_v [34], the pre-adapted *Chloridium ellipsoideum* [53] identified in our system supported a progressive increase in CO_2 and H_2S EC. This suggests that the microbial community effectively adapted to rising H_2S loads without experiencing inhibition, indicating a higher tolerance to sulfide exposure. This remarkable tolerance stems from the inoculum's history, having been long-term adapted to H_2S concentrations up to 5000 ppm_v in a pilot high-rate algal pond devoted to biogas upgrading, likely due to strong selective pressure favoring resilient strains. While most *Chlorella sp.* studies report performance at significantly lower H_2S concentrations ($< 8000 \text{ ppm}_v$), direct comparative data for *Chloridium ellipsoideum* at extremely high levels like those in vinasse off-gas are limited in literature, underscoring the novelty of our work.

The system exhibited a maximum H_2S -EC of $30.3 \text{ gS-H}_2\text{S m}^{-3} \text{ h}^{-1}$ during Stage III, achieving 100% H_2S -RE (Fig. 2 b), which positions it as highly competitive relative to previously reported biotrickling filters devoted to acidogenic off-gas acidification under both aerobic and anoxic conditions. This performance is particularly notable considering the extreme H_2S concentrations ($50,000 \text{ ppm}_v$) treated, a level significantly higher than typically reported in literature. For instance, in aerobic biological systems, Kim et al. [39] reported an EC of $8.0 \text{ gS-H}_2\text{S m}^{-3} \text{ h}^{-1}$ with 52% H_2S -RE, significantly lower than the performance observed in the current study. Similarly, Vikromvarasiri et al. [87] achieved a maximum EC of $78.6 \text{ gS-H}_2\text{S m}^{-3} \text{ h}^{-1}$ with H_2S -RE ranging from 40% to 92% under increasing EBRTs, both significantly lower in consistency than our system's complete H_2S removal. While Montebello et al. [55] reported a higher EC of $51.5 \text{ gS-H}_2\text{S m}^{-3} \text{ h}^{-1}$ with complete H_2S removal in an aerobic BTF, their study highlighted the detrimental

buildup of biosulfur and extensive biomass colonization on packing material, hindering long-term liquid distribution and oxygen penetration. Similarly, anoxic BTFs (e.g., [43], $54.5 \text{ gS-H}_2\text{S m}^{-3} \text{ h}^{-1}$, 100% H_2S removal; [79], $47.4 \text{ gS-H}_2\text{S m}^{-3} \text{ h}^{-1}$, 84.4% RE) face limitations like slower sulfide oxidation, sulfur accumulation, biofilm overgrowth, reliance on external electron acceptors, and higher operational costs [2]. The sustained superior performance observed in this study, particularly under such extreme H_2S loads, directly resulted from the effective internal process oxygenation by microalgae within the unique bubble column reactor design. This design inherently overcomes the oxygen mass transfer limitations commonly encountered in conventional packed-bed BTFs, thereby preventing elemental sulfur accumulation and ensuring long-term stability [72,92].

The gas composition of the treated off-gas further confirmed the efficiency of the algal-bacterial photobioreactor. Oxygen levels in the outlet gas increased from $1.2 \pm 0.2\%$ to $22.0 \pm 5.3\%$ (Fig. 2 c-d), demonstrating active oxygen generation by microalgae. Simultaneously, the outlet CO_2 concentrations dropped to $1.3 \pm 0.7\%$, which highlighted the sustained CO_2 biofixation. Crucially, the consistently high dissolved oxygen (DO) levels prevailing in the cultivation broth (averaging 15.0 mg L^{-1}), ensured that sulfide oxidation remained efficient throughout the operational period, preventing the accumulation of inhibitory or clogging-related intermediate sulfur species. Additionally, TDS in the cultivation broth remained below quantification limits, confirming that H_2S was fully oxidized to sulfate without accumulation of intermediate sulfur species. The system effectively handled elevated H_2S concentrations in the acidogenic off-gas, demonstrating the feasibility of using a combined microalgal-bacterial approach to mitigate the environmental impact of high-strength H_2S streams from sugarcane biorefineries.

A comparison with previous studies (Table S1 - Supplementary Material, Fig. 3 a) highlights the exceptional performance of the algal-bacterial photobioreactor herein tested under extreme H_2S loads. While most studies reported nearly complete H_2S removal ($\sim 100\%$) at significantly lower H_2S concentrations ($< 8000 \text{ ppm}_v$), our system effectively treated acidogenic off-gas with an exceptionally high H_2S concentration ($50,000 \text{ ppm}_v$). Additionally, previous studies reported H_2S -ECs typically between 0.1 and $17.9 \text{ gS-H}_2\text{S m}^{-3} \text{ h}^{-1}$ [12,3,48,71], with only a few reaching values above $10.0 \text{ gS-H}_2\text{S m}^{-3} \text{ h}^{-1}$ [25,41,70,86]. In contrast, this study achieved the highest EC (up to $30.3 \text{ gS-H}_2\text{S m}^{-3} \text{ h}^{-1}$) reported in the literature for CMB systems, while still maintaining complete H_2S -RE. In this case, the fine bubble dispersion mechanism further enhanced gas-liquid contact and promoted uniform exposure to the microbial community, contributing to the efficient detoxification of sulfide.

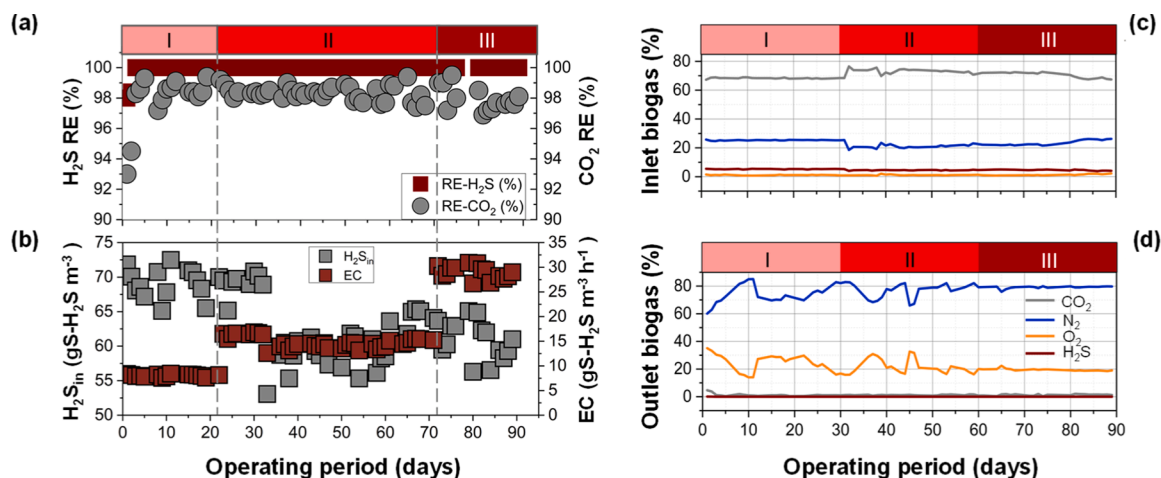


Fig. 2. Time course of (a) H_2S and CO_2 removal efficiencies (REs), (b) inlet H_2S concentrations (H_2S_{in}) and elimination capacities (ECs), (c) inlet acidogenic off-gas content, and (d) outlet off-gas concentrations.

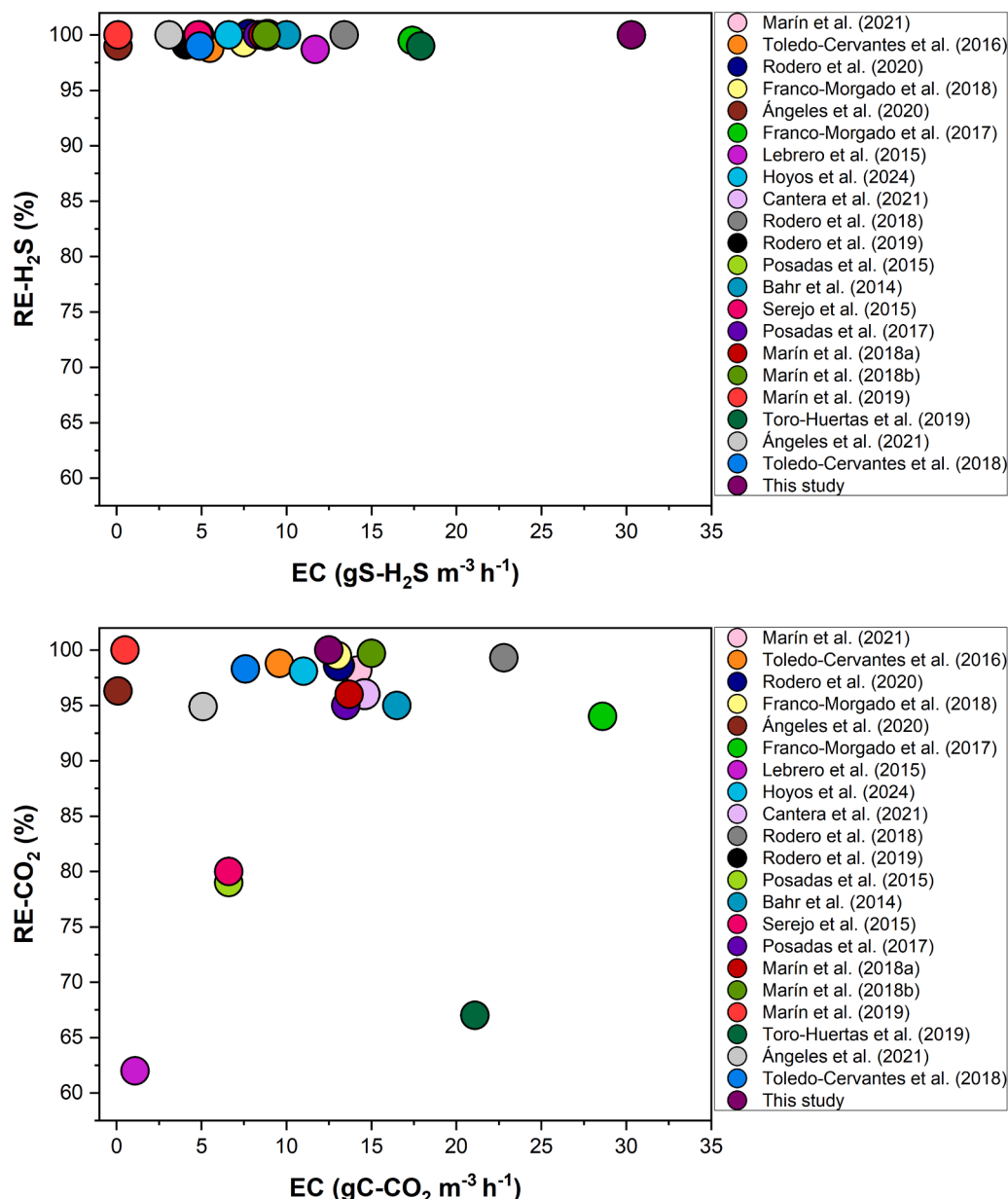


Fig. 3. Summary of the performance of previous studies assessing the simultaneous removal of (a) H_2S and (b) CO_2 in pilot and lab-scale algal photobioreactors. Legend: RE – removal efficiency, LR – loading rate. Parameters were directly taken from the referenced studies when reported. When not explicitly provided, they were calculated based on the available data within the respective papers.

CO_2 -RE in microalgal systems is typically influenced by multiple factors, including CO_2 -LR, IC availability, illumination conditions, and wastewater characteristics. As shown in Fig. 3 b, most studies in the literature have reported CO_2 -ECs below $15 \text{ gC-CO}_2 \text{ m}^{-3} \text{ h}^{-1}$, achieving CO_2 -REs values ranging between 62 % and 99.7 %. On the other hand, a few studies have successfully reached higher ECs while maintaining relatively high CO_2 -REs (Table S1- Supplementary Material). Franco-Morgado et al. [25] achieved a maximum EC of $28.6 \text{ gC-CO}_2 \text{ m}^{-3} \text{ h}^{-1}$ at a CO_2 -RE of 94 % under continuous illumination in a 180 L HRAP, which was attributed to the high IC concentrations ($1500\text{--}2000 \text{ mg-IC L}^{-1}$) in the cultivation broth, which sustained a high photosynthetic activity and stabilized pH at 9.5. Maximum ECs of 22.8 and $36.3 \text{ gC-CO}_2 \text{ m}^{-3} \text{ h}^{-1}$ were reported by Rodero et al. [70,69], respectively, associated with CO_2 -REs above 95 %. However, a decline in CO_2 -RE from 99.3 % to 30.8 % under semi-continuous illumination in a 180 L HRAP were also reported by Rodero et al. [70] due to reduction in IC availability from

1500 to 100 mg-IC L^{-1} . Similarly, Rodero et al. [69] observed CO_2 -REs ranging from 56.4 % to 99.1 %, depending on wastewater type, with centrate yielding the highest RE due to its higher pH and IC availability, while variations in HRT and biogas flowrate exerted a negligible effect on CO_2 removal. The present study achieved CO_2 -LR up to $12.5 \text{ gC-CO}_2 \text{ m}^{-3} \text{ h}^{-1}$ with sustained 98 % CO_2 -RE, suggesting that effective IC management, pH control, and optimized reactor design mitigated carbon limitation effects, especially under extreme CO_2 and H_2S loads. These findings underscore the importance of maintaining adequate alkalinity and mass transfer efficiency to enhance CO_2 solubilization and uptake by microalgal-bacterial communities.

3.2. Environmental conditions and system stability

During Stage I, the average pH levels in the cultivation broth of the algal pond and AC were 9.7 ± 0.1 and 9.6 ± 0.1 , respectively (Fig. 4 a). As the H_2S -LR increased from 8.1 ± 0.2 (Stage I) to $14.7 \pm 1.1 \text{ gS-H}_2\text{S}$

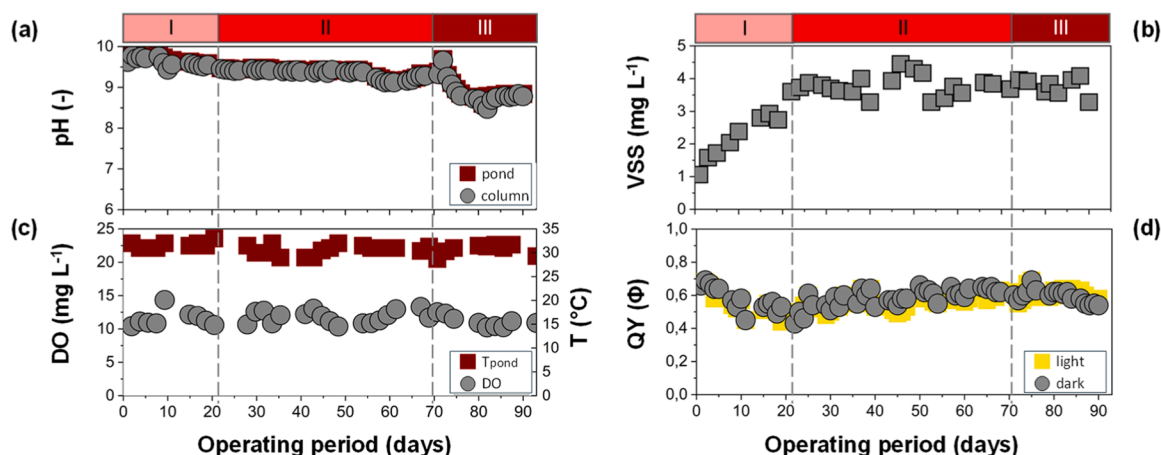


Fig. 4. Time course of (a) pH, (b) volatile suspended solids (VSS), (c) dissolved oxygen (DO) and temperature (T), and (d) quantum yield (QY).

$\text{m}^{-3} \text{h}^{-1}$ (Stage II), these pH values slightly decreased to 9.4 ± 0.1 and 9.3 ± 0.1 , respectively, with minimum pH values of 8.9 ± 0.3 and 8.8 ± 0.3 observed at the highest H_2S -LR ($29.0 \pm 1.3 \text{ gS-H}_2\text{S m}^{-3} \text{h}^{-1}$). Although lower CO_2 and H_2S removal efficiencies are commonly reported in CMB systems at reduced pH levels (~ 9.0) and IC concentrations ($< 500 \text{ mg L}^{-1}$) [11,70], this study achieved an effective buffering capacity critical for maintaining a balance between microbial activity and $\text{CO}_2/\text{H}_2\text{S}$ mass transfer in the bubble column, thereby ensuring long-term stability in treatment of the acidogenic off-gas. The robust pH stability observed, despite increasing proton generation from H_2S oxidation, highlights the efficacy of the system's buffering capacity. This stability is paramount for sustaining optimal conditions for both microalgal photosynthetic activity and the enzymatic functions of SOB. The increase in IC concentrations in the cultivation broth from $1853 \pm 166 \text{ mg L}^{-1}$ in Stage II to $3412 \pm 251 \text{ mg L}^{-1}$ in Stage III directly correlates with elevated CO_2 sequestration rates, indicating that higher gaseous CO_2 inputs effectively enhanced dissolved inorganic carbon availability, which was then efficiently biofixed by the microalgae.

In Stage I, DO levels were slightly low, averaging around 10.0 mg L^{-1} , coinciding with the early establishment of the microalgal-bacterial community (Fig. 4 c). As the system stabilized in Stages II and III, DO levels rose to an average of 15.0 mg L^{-1} (maximum of 20.1 mg L^{-1}), among the highest reported for indoor systems and comparable to or exceeding those observed in outdoor systems ($0.9\text{--}25.0 \text{ mg L}^{-1}$) [3,51,50,69]. Indoor systems typically exhibit more controlled DO conditions ($0.7\text{--}20.4 \text{ mg L}^{-1}$) [26,83,84,85], whereas outdoor systems showed greater variability due to natural fluctuations in light and temperature [36,48,61]. The consistently high DO values (averaging 15.0 mg L^{-1}) are a critical operational achievement, directly linked to the microalgae's vigorous photosynthetic activity and their inherent tolerance to high H_2S loads. This ample oxygen supply ensured a complete sulfide oxidation to sulfate, preventing oxygen limitations that often lead to elemental sulfur formation and reactor clogging, as indicated by lower DO values ($\sim 0.7\text{--}6.0 \text{ mg L}^{-1}$) in some studies [41, 68]. Higher DO levels ($> 10.0 \text{ mg L}^{-1}$) are indeed known to support complete sulfide oxidation [4,71], confirming the efficacy of our system's internal oxygenation.

Quantum yield (QY) values, a proxy of photosynthetic efficiency within the HRAP, remained constant at approximately 0.6 (Fig. 4 d), suggesting effective adaptation of the microalgae to the continuous illumination, thereby optimizing light utilization for photosynthesis. The cultivation broth and ambient temperatures were consistently maintained at $30.8 \pm 0.9^\circ\text{C}$ and $27.0 \pm 1.0^\circ\text{C}$, respectively, ensuring optimal conditions for the microalgal-bacterial synergism and preventing thermal stress. The inherent tolerance of *Chloroidium ellipsoideum* in maintaining high photosynthetic activity and robust biomass growth even under extremely high H_2S concentrations was key to continuously

supplying oxygen above saturation levels to the cultivation broth, a vital factor for the subsequent biological sulfide oxidation.

3.3. Inorganic carbon, sulfate and nitrogen fate

The interplay between IC and sulfate accumulation plays a crucial role in determining system stability, particularly in CMB systems exposed to extreme H_2S loads, thus directly underpins the exceptionally high removal efficiencies observed. SOB oxidize H_2S to sulfate via intermediate sulfur species (S^0 , S_2O_3), generating protons that can lead to acidification if not counteracted by a sufficient IC buffer capacity [20]. Despite the increasing sulfate accumulation in the cultivation broth, the consistently high pH (> 8.8) observed in this study suggests that IC played a major role in stabilizing system alkalinity. This aligns with previous studies reporting that CO_2 removal is highly influenced by alkalinity [61], while other parameters such as temperature [70], biomass productivity [49], $\text{H}_2\text{S}/\text{CO}_2$ absorption units [68], illumination regime [25], open/closed photobioreactors configurations [3,84], biogas supply regime [4], gas-liquid flow configurations [83] or biogas recirculation [36] play a minor role in the quality of the biogas. The combined effect of high IC availability (Fig. 5 a) and elevated O_2 concentrations likely stabilized the pH and enabled a complete sulfide oxidation without triggering sulfate reduction. This sustained high IC availability was predominantly driven by the significant CO_2 partial pressure from the off-gas, particularly as the gaseous CO_2 loading rates increased across the operational stages.

Microalgal CO_2 uptake is another key factor influencing IC dynamics. While microalgae actively assimilate dissolved CO_2 , potentially depleting IC and raising pH [35], our findings indicate that CO_2 availability remained sufficient to prevent imbalances. The use of a gas mixture with a high CO_2 concentration ($> 70\%$), compared to the $\sim 30\%$ reported in similar systems (Supplementary Material, Table S1), likely sustained IC levels and prevented excessive pH fluctuations. If CO_2 assimilation outpaced IC replenishment, pH might rise excessively (> 10), leading to carbonate precipitation (e.g., CaCO_3), which could indirectly affect sulfate solubility and microbial activity [91]. While no visible precipitates were observed in this study, future studies should explore whether undetectable carbonate formation could influence long-term system performance. Ultimately, the high removal efficiencies for both H_2S and CO_2 are a direct consequence of the synergistic combination of the *Chloroidium ellipsoideum*'s high tolerance to elevated H_2S , its sustained oxygen production, the efficient activity of SOB, and the effective management of IC and pH dynamics driven by the system's robust design and the unique composition of the vinasse off-gas.

Sulfate accumulation remained within a controlled range ($186\text{--}1170 \text{ mgS-SO}_4^{2-} \text{ L}^{-1}$) of non-inhibitory concentrations throughout the experiment (Fig. 5 b). Sulfate concentrations increased in Stages I ($186\text{--}259$

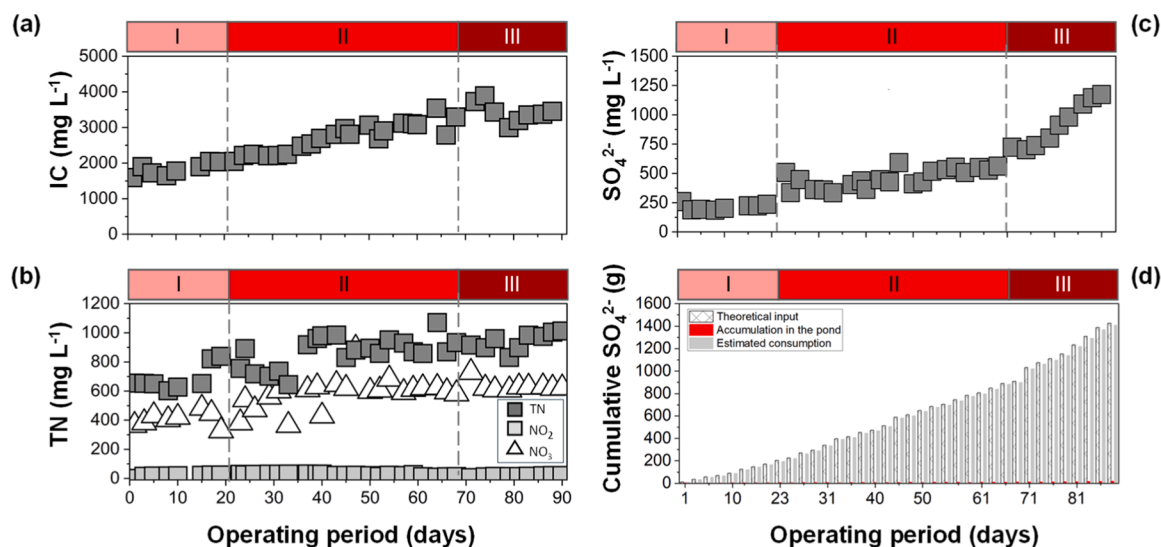


Fig. 5. Time course of the concentrations of (a) inorganic carbon, (b) total nitrogen, (c) sulfate (SO_4^{2-}), and (d) cumulative SO_4^{2-} .

$\text{mgS-SO}_4^{2-} \text{ L}^{-1}$) and II ($334 - 591 \text{ mg L}^{-1}$) as a response of an active H_2S oxidation. The highest sulfate accumulation in the pond was observed in Stage III with H_2S -LRs ranging from 700 to $1170 \text{ mgS-SO}_4^{2-} \text{ L}^{-1}$. Notably, a comprehensive sulfur mass balance revealed that up to 99 % of the theoretical sulfate entering the system (from both H_2S gas flow and $\text{MgSO}_4 \cdot 7\text{H}_2\text{O}$ from the mineral solution) was actively consumed by the microalgal-bacterial consortium for biomass growth, demonstrating exceptional sulfur assimilation efficiency. In Stage I, biomass growth rates were higher compared to Stages II and III (Fig. 4 b), corroborating the enhanced sulfate assimilation, ranging from 67 % to 98 % of the total theoretical sulfate input (Fig. 5 d). When biomass reached stable levels in the pond at $3.8 \pm 0.2 \text{ g-VSS L}^{-1}$, sulfate assimilation remained stable (99 %). Thus, sulfate assimilation by microalgae into sulfur-containing biomolecules likely played a significant role in maintaining sulfate balance [82]. Regular biomass removal from the cultivation broth further contributed to the stabilization of sulfate concentrations by eliminating the sulfur incorporated into the algal protein. Together, these processes likely ensured a controlled sulfur cycle within the system. This stability is critical because excessive sulfate accumulation could compete with bicarbonate for transporters, potentially affecting photosynthesis in microalgae and cyanobacteria. While SulP-type transporters have been implicated in bicarbonate-sulfate competition [65], their role in microalgae remains poorly characterized. In any case, the stable quantum yield ($\text{QY} \sim 0.6$) and increased biomass production indicate that sulfate levels did not negatively impact photosynthetic performance, although further studies are needed to assess sulfate-bicarbonate competition at the transporter level.

Finally, nitrate dynamics further support the hypothesis of a biologically stable system (Fig. 5 c). In the absence of organic carbon sources and under continuous illumination, microalgae were the primary nitrate consumers, likely assimilating NO_3^- via nitrate reductase enzymes and incorporating nitrogen into cellular components such as amino acids and proteins [13]. Since O_2 levels remained above saturation in the cultivation broth, the contribution of nitrate to bacterial H_2S oxidation via autotrophic denitrification was likely negligible. The low concentrations of intermediate oxidized nitrogen species, such as nitrite (NO_2^-), suggest an efficient nitrogen utilization, mitigating potential inhibitory effects on photosynthesis [33]. Nitrate removal efficiency ($\text{NO}_3\text{-RE}$) reached 39.4 %, 64.7 %, and 70.4 % by the end of Stages I, II, and III, respectively, corresponding to a removal rate of $5.2 \pm 0.1 \text{ gN-NO}_3 \text{ m}^{-3} \text{ d}^{-1}$ across all stages. Similar $\text{NO}_3\text{-RE}$ values (45–70 %) were reported by Rocher-Rivas et al. [68] in an HRAP fed with nitrate-rich MSM. However, their system operated at a higher nitrate

removal rate (16 ± 4 and $25 \pm 5 \text{ gN-NO}_3 \text{ m}^{-3} \text{ d}^{-1}$) due to the higher biomass concentration (up to 1.3 g-VSS L^{-1}) and $\text{CO}_2\text{-LR}$ ($1422\text{--}4267 \text{ g m}^{-3} \text{ h}^{-1}$). These results indicate that the significantly lower nitrate inputs (~ 5 -fold lower) in this study were sufficient to sustain microalgal growth, highlighting the potential for reducing operational costs associated with nitrate supplementation. Maximum nitrogen removal rates of $23.9 \text{ gN m}^{-3} \text{ d}^{-1}$ [89], $17.0 \text{ gN m}^{-3} \text{ d}^{-1}$ [8], and $9.0 \text{ gN m}^{-3} \text{ d}^{-1}$ [70] were reported in photosynthetic systems fed using real ammonium-rich centrate as nutrient medium for biogas purification and upgrading. Overall, it was confirmed that CMB systems devoted to H_2S -rich acidogenic off-gas support $\text{NO}_3\text{-RE}$ s of up to 70 %, showcasing a balance between sufficient CO_2 for photosynthesis and stable nitrogen assimilation, without requiring external carbon supplementation.

3.4. Microbial growth response to operational conditions

The abundance of the algal-bacterial biomass evolved throughout the three operational stages, reflecting the consortium's adaptation to increasing off-gas flow rates. Microalgae abundance at the end of Stage I was 6.94×10^9 individuals per liter (ind. L^{-1}) or $3.49 \times 10^{11} \mu\text{m}^{-3} \text{ L}^{-1}$, followed by a decline in Stage II ($5.61 \times 10^9 \text{ ind. L}^{-1}$ or $2.82 \times 10^{11} \mu\text{m}^{-3} \text{ L}^{-1}$) and a subsequent increase in Stage III ($1.05 \times 10^{10} \text{ ind. L}^{-1}$ or $5.27 \times 10^{11} \mu\text{m}^{-3} \text{ L}^{-1}$). These dynamic shifts in abundance are indicative of the consortium's adaptive strategies, driven by the evolving environmental pressures of increasing pollutant loads, and demonstrate the resilience of the combined system. The observed changes were likely influenced by sulfide oxidation activity, IC availability, and the capacity of the system to handle escalating H_2S and CO_2 loads.

Notably, this study implemented a zero-effluent operational strategy, meaning no biomass removal was conducted, an approach distinct from previous CMB systems where periodical biomass harvesting was essential to maintain high biomass productivity [36,48,50,61,63,83,85]. This strategy successfully maximized biomass retention within the reactor, contributing to the overall valorization of the off-gas pollutants. The stability of quantum yield ($\text{QY} \sim 0.6$) further suggests that photosynthetic efficiency was not negatively impacted, despite the system's escalating sulfide oxidation demand. The decrease in microbial abundance during Stage II may reflect a transient stress response due to the rising H_2S and CO_2 inputs, requiring an adaptive shift in microbial activity. However, the substantial increase observed in Stage III strongly suggests that the algal-bacterial consortium successfully acclimated to these more extreme conditions, demonstrating remarkable resilience

and adaptive capacity under sustained high loads. The concurrent stability in sulfate accumulation and efficient nitrate assimilation further indicate that microalgae effectively incorporated available nutrients, preventing inhibitory effects from residual sulfide or excessive sulfate buildup, which is vital for sustained growth.

These findings highlight the critical role of algal-bacterial interactions in maintaining system resilience. The ability of the microbial consortium to sustain growth under increasing gas loads reinforces the stability of the photobioreactor, ensuring efficient H₂S removal and CO₂ assimilation while maintaining a balanced microbial ecosystem.

3.5. The path forward

Despite its effectiveness, the CMB system presents operational challenges, primarily related to pH control. The bacterial oxidation of H₂S releases protons, leading to an acidification of the cultivation broth that can inhibit microbial activity [42]. While microalgal CO₂ fixation thrives at alkaline pH (8.2–8.7) [37], SOB perform optimally near neutrality [88], creating a delicate balance. Maintaining stability typically requires IC supplementation, yet this incurs significant operational costs, limiting large-scale application [70,71].

The economic feasibility of CMB systems remains a challenge, as maintaining alkalinity through chemical supplementation significantly increases operating costs. To address this, alternative buffering strategies, such as the use of digestates, which offers renewable sources of IC and nutrients, have been explored [1,12,26,36,47,61,63,64,69,70,83,84]. However, the average IC concentration in centrate ranges from 450 to 600 mg-IC L⁻¹ and is reported in the literature as insufficient to meet the demands of CMB systems, requiring additional supplementation with NaHCO₃ and Na₂CO₃ to reach values close to 2,000 mg-IC L⁻¹ [70]. Most studies utilizing these digestate/centrate were conducted at the laboratory scale with synthetic biogas simulating conventional methanogenic biogas (70 % CH₄ and < 0.5 % H₂S), limiting their direct extrapolation to high-H₂S industrial scenarios [51,50,61,70].

In summary, this approach limits the extrapolation of results to industrial scenarios where biogas contain high H₂S concentrations (such as those from acidogenic-sulfidogenic reactors), requiring more efficient control of medium acidification resulting from increased H₂S oxidation rates and greater microbial resilience to maintain system stability. Therefore, operational conditions more representative of sulfide-rich biogas remain a scientific gap with direct implications for the scalability of these systems. To enhance the economic viability of the process, future research should focus on cost-effective alternatives for IC supplementation. One avenue is the use of biodigested sugarcane vinasse from single or two-phase (acidogenic-methanogenic) AD systems. This strategy remains largely unexplored and could provide a sustainable nutrient and alkalinity source for CMB systems.

While microalgal cultivation is feasible in various industrial and domestic effluents [38,52,57,62], raw sugarcane vinasse presents challenges such as low pH (4.0–4.5), high organic load (25–40 kg COD_r m⁻³ h⁻¹), and high turbidity due to melanoidins, which can limit light penetration and hinder photosynthetic activity [23,30]. Anaerobically

biodigested sugarcane vinasse, however, offers an improved pH and alkalinity profile, making it a particularly promising and viable alternative for CMB system operation that could reduce reliance on external alkalinity sources [52,78]. Table 1 presents reference values from the literature for partial alkalinity (PA) concentrations obtained from high-rate methanogenic systems treating sugarcane vinasse.

Notably, two-phase AnSTBR reactors with sulfate removal in the acidogenic phase exhibit significantly higher PA (8,700–9,100 mg-CaCO₃ L⁻¹) and IC concentrations (2,090–2,180 mg-IC L⁻¹) compared to single-phase UASB reactors [28,31]. These findings suggest that biodigested vinasse could stabilize pH when treating high concentrations, potentially reducing or eliminating external alkaline supplementation. Future research should assess the long-term effects of biodigested vinasse on CMB system performance, particularly its impact on microbial community stability, nutrient dynamics, and by-product formation. Additionally, studies should investigate the integration of biodigested vinasse into large-scale biorefinery operations, considering economic feasibility, regulatory constraints, and environmental sustainability.

While the present study robustly demonstrated the high-efficiency removal of H₂S and CO₂ from the gas phase, the liquid effluent from our system, though transforming gaseous pollutants into a soluble and nutrient-rich stream, still contains elevated levels of certain compounds (e.g., inorganic carbon, nitrate). It is acknowledged that further downstream treatment or valorization steps may be required for this liquid phase within a complete biorefinery scheme, a promising area for future investigation beyond the scope of this work. The adoption of these strategies could align with circular economy principles, promoting the reuse of agricultural residues while reducing waste disposal and mitigating environmental impacts. By also incorporating biodigested vinasse as a sustainable water, alkalinity and nutrient source, CMB systems could contribute not only to H₂S mitigation but also to broader goals of reducing GHG emissions and eutrophication in sugarcane biorefineries.

4. Conclusions

This study demonstrated the effectiveness of a novel CMB system for simultaneous H₂S and CO₂ removal from acidogenic off-gas generated during vinasse fermentation. The system achieved 100 % H₂S removal and 98.2 % CO₂ biofixation, maintaining a robust performance even under increased gas flow rates in the tested range. Microbial adaptation to 72 gS-H₂S m⁻³ led to a 4.5 × biomass increase and sustained sulfur oxidation. The system's efficiency was largely driven by optimized alkalinity (1.8–3.4 g L⁻¹), controlled sulfate accumulation (186–1170 mgS-SO₄²⁻ L⁻¹), and reduced nitrate input (5 × lower), compared to conventional CMB systems, reinforcing its potential economic feasibility. The maximum elimination capacity of 30.3 gS-H₂S m⁻³ h⁻¹ herein obtained position the CMB approach as a high-competitive alternative to traditional gas purification technologies, offering both cost savings and environmental benefits within a circular bioeconomy framework. Moving forward, further studies should focus on biomass harvesting optimization, system scalability, and the potential use of biodigested vinasse as a pH stabilizer. Refining inorganic carbon

Table 1
Alkalinization of high-rate methanogenic systems in sugarcane vinasse processing.

AD setup	Sulfate removal	Reactor type	PA (mg-CaCO ₃)	IC ^a (mg L ⁻¹)	OLR (kgCOD m ⁻³ d ⁻¹)	NaHCO ₃ ^b (g g ⁻¹ COD _t)	Reference
Single-Phase AD	No	UASB	4,000–4,500	960–1,080	20	0.35	[24]
	No	UASB	3,000–4,000	720–960	20	0.18	[24]
Two-Phase AD	No	AnSTBR	6,000	1,418	20	0.22	[31]
	Yes ^c	AnSTBR	8,700–9,100	2,090–2,180	20	0.25	[28]

Abbreviations: AnSTBR, Anaerobic structured-bed reactor, PA – partial alkalinity, OLR – organic loading rate, COD – chemical oxygen demand, IC – inorganic carbon, UASB – Upflow Anaerobic sludge blanket. ^a Conversion based on the following stoichiometry: 2 HCO₃⁻ + Ca → CaCO₃ + CO₂ + H₂O. ^b Bicarbonate dosage in the methanogenic stage. ^c Sulfate removal in the acidogenic stage.

supplementation strategies could further enhance CO₂ sequestration efficiency in biorefinery facilities, while reducing operational costs.

Environmental implication

Sugarcane biorefineries generate hazardous emissions, particularly hydrogen sulfide (H₂S) and carbon dioxide (CO₂), during vinasse fermentation, posing environmental and occupational risks. The combined microalgal-bacterial (CMB) system offers a biologically driven alternative to conventional scrubbing, achieving near-complete removal of both gases without harmful by-products. Through H₂S oxidation and CO₂ fixation, it mitigates pollution, odor, and corrosion, while reducing the carbon footprint. Sulfate accumulation and biomass growth support nutrient recovery and waste valorization. Operating with minimal energy and inputs, the CMB system provides a scalable, low-cost solution for biogas upgrading, promoting environmental protection and industrial sustainability.

CRedit authorship contribution statement

André do Vale Borges: Conceptualization, Investigation, Writing, Methodology, Software, Writing – original draft. **Andrés Felipe Torres Franco:** Conceptualization, Methodology, Data curation, Validation. **Márcia Helena Rissato Zamariolli Damianovic:** Conceptualization, Funding acquisition, Project administration, Resources, Validation. **Raúl Muñoz:** Conceptualization, Supervision, Funding acquisition, Project administration, Data curation, Writing – review & editing, Validation.

Declaration of Competing Interest

The authors declare that they have no known competing financial interests or personal relationships that could have appeared to influence the work reported in this paper.

Acknowledgments

This work was supported by the São Paulo Research Foundation [grant numbers 2021/15245–5; 2023/04885–9]. The authors also acknowledge the support of the regional Government of Castilla y León (UIC 379).

Appendix A. Supporting information

Supplementary data associated with this article can be found in the online version at [doi:10.1016/j.jhazmat.2025.139539](https://doi.org/10.1016/j.jhazmat.2025.139539).

Data Availability

Data will be made available on request.

References

- Alcántara, C., García-Encina, P.A., Muñoz, R., 2015. Evaluation of the simultaneous biogas upgrading and treatment of centrates in a high-rate algal pond through C, n and p mass balances. *Water Sci Technol* 72 (1), 150–157. <https://doi.org/10.2166/wst.2015.198>.
- Almenglo, F., González-Cortés, J.J., Ramírez, M., Cantero, D., 2023. Recent advances in biological technologies for anoxic biogas desulfurization. *Chemosphere* 321, 138084. <https://doi.org/10.1016/j.chemosphere.2023.138084>.
- Ángeles, R., Arnaiz, E., Gutiérrez, J., Sepúlveda-Muñoz, C.A., Fernández-Ramos, O., Muñoz, R., et al., 2020. Optimization of photosynthetic biogas upgrading in closed photobioreactors combined with algal biomass production. *J Water Process Eng* 38, 101554. <https://doi.org/10.1016/j.jwpe.2020.101554>.
- Ángeles, R., Vega-Quiel, M.J., Batista, A., Fernández-Ramos, O., Lebrero, R., Muñoz, M., 2021. Influence of biogas supply regime on photosynthetic biogas upgrading performance in an enclosed algal-bacterial photobioreactor. *Algal Res* 57, 102350. <https://doi.org/10.1016/j.algal.2021.102350>.
- APHA, AWWA, WEF, 2012. *Standard Methods for Examination of Water and Wastewater*, 22 nd. ed. APHA, Washington, D.C.
- Aquino, S.De, Fuess, L.T., Pires, E.C., 2017. Bioreactor technology media arrangement impacts cell growth in anaerobic fixed-bed reactors treating sugarcane vinasse: structured vs. Randomic biomass immobilization. *Bioresour Technol* 235, 219–228. <https://doi.org/10.1016/j.biortech.2017.03.120>.
- Azizi, S.M.M., Zakaria, B.S., Haffiez, N., Niknejad, P., Dhar, B.R., 2022. A critical review of prospects and operational challenges of microaeration and iron dosing for *in-situ* biogas desulfurization. *Bioresour Technol Rep* 20, 101265. <https://doi.org/10.1016/j.biteb.2022.101265>.
- Bahr, M., Díaz, I., Domínguez, A., Sánchez, A.G., Muñoz, R., 2014. Microalgal-biotechnology as a platform for an integral biogas upgrading and nutrient removal from anaerobic effluents. *Environ Sci Technol* 48 (1), 573–581. <https://doi.org/10.1021/es403596m>.
- Borges, A.V., Damianovic, M.H.R.Z., Torre, R.M., 2025. Assessment of aerobic-anoxic biotrickling filtration for the desulfurization of high-strength H₂S streams from sugarcane vinasse fermentation. *J Hazard Mater* 489, 137696. <https://doi.org/10.1016/j.jhazmat.2025.137696>.
- Borges, A.V., Fuess, L.T., Takeda, P.Y., Rogeri, R.C., Saia, F.T., Gregoracci, G.B., et al., 2025. Unleashing the full potential of vinasse fermentation in sugarcane biorefineries. *Renew Sustain Energy Rev* 208, 115096. <https://doi.org/10.1016/j.rser.2024.115096>.
- Bose, A., Lin, R., Rajendran, K., O'Shea, R., Xia, A., Murphy, J.D., 2019. How to optimise photosynthetic biogas upgrading: a perspective on system design and microalgae selection. *Biotechnol Adv* 37 (8), 107444. <https://doi.org/10.1016/j.biotechadv.2019.107444>.
- Cantera, S., Fischer, P.Q., Sánchez-Andrea, I., Marín, D., Sousa, D.Z., Muñoz, R., 2021. Impact of the algal-bacterial community structure, physio-types and biological and environmental interactions on the performance of a high-rate algal pond treating biogas and wastewater. *Fuel* 302, 121148. <https://doi.org/10.1016/j.fuel.2021.121148>.
- Chen, H., Wang, Q., 2020. Microalgae-based nitrogen bioremediation. *Algal Res* 46, 101775. <https://doi.org/10.1016/j.algal.2019.101775>.
- Chen, H., Wu, J., Liu, B., Li, Y.Y., Yasui, H., 2019. Competitive dynamics of anaerobes during long-term biological sulfate reduction process in a UASB reactor. *Bioresour Technol* 280, 173–182. <https://doi.org/10.1016/j.biortech.2019.02.023>.
- Costanzo, N.D., Di Capua, F., Cesaro, A., Carraturo, F., Salamone, M., Guida, M., et al., 2024. Headspace micro-oxygenation as a strategy for efficient biogas desulfurization and biomethane generation in a centralized sewage sludge digestion plant. *Biomass Bioenergy* 183, 107151. <https://doi.org/10.1016/j.biombioe.2024.107151>.
- Culaba, A.B., Mayol, A.P., San Juan, J.L.G., Ubando, A.T., Bandala, A.A., Concepcion Ii, R.S., et al., 2023. Design of biorefineries towards carbon neutrality: a critical review. *Bioresour Technol* 369, 128256. <https://doi.org/10.1016/j.biortech.2022.128256>.
- Dada, O.I., Yu, L., Neibergs, S., Chen, S., 2025. Biodesulfurization: effective and sustainable technologies for biogas hydrogen sulfide removal. *Renew Sustain Energy Rev* 209, 115144. <https://doi.org/10.1016/j.rser.2024.115144>.
- Das, J., Ravishankar, H., Lens, P.N., 2022. Biological biogas purification: recent developments, challenges and future prospects. *J Environ Manag* 304, 114198. <https://doi.org/10.1016/j.jenvman.2021.114198>.
- de Oliveira, B.G., Carvalho, J.L.N., Cerri, C.E.P., Cerri, C.C., Feigl, B.J., 2015. Greenhouse gas emissions from sugarcane vinasse transportation by open channel: a case study in Brazil. *J Clean Prod* 94, 102–107. <https://doi.org/10.1016/j.jclepro.2015.02.025>.
- De Rink, R., Klok, J.B., Van Heeringen, G.J., Sorokin, D.Y., Ter Heijne, A., Zeijlmaker, R., et al., 2019. Increasing the selectivity for sulfur formation in biological gas desulfurization. *Environ Sci Technol* 53 (8), 4519–4527. <https://doi.org/10.1021/acs.est.8b06749>.
- Del Nery, V., Alves, I., Damianovic, M.H.R.Z., Pires, E.C., 2018. Hydraulic and organic rates applied to pilot scale UASB reactor for sugar cane vinasse degradation and biogas generation. *Biomass Bioenergy* 119, 411–417. <https://doi.org/10.1016/j.biombioe.2018.10.002>.
- Egger, F., Hülsen, T., Tait, S., Batstone, D.J., 2020. Autotrophic sulfide removal by mixed culture purple phototrophic bacteria. *Water Res* 182, 115896. <https://doi.org/10.1016/j.watres.2020.115896>.
- Escudero, A., Blanco, F., Lacalle, A., Pinto, M., 2014. Ammonium removal from an anaerobically treated effluent by *chlamydomonas acidophila*. *Bioresour Technol* 153, 62–68. <https://doi.org/10.1016/j.biortech.2013.11.076>.
- Ferraz-Júnior, A.D.N.F., Koyama, M.H., de Araújo Júnior, M.M., Zaiat, M., 2016. Thermophilic anaerobic digestion of raw sugarcane vinasse. *Renew Energy* 89, 245–252. <https://doi.org/10.1016/j.renene.2015.11.064>.
- Franco-Morgado, M., Alcántara, C., Noyola, A., Muñoz, R., González-Sánchez, A., 2017. A study of photosynthetic biogas upgrading based on a high-rate algal pond under alkaline conditions: influence of the illumination regime. *Sci Total Environ* 592, 419–425. <https://doi.org/10.1016/j.scitotenv.2017.03.077>.
- Franco-Morgado, M., Toledo-Cervantes, A., González-Sánchez, A., Lebrero, R., Muñoz, R., 2018. Integral (VOCs, CO₂, mercaptans and H₂S) photosynthetic biogas upgrading using innovative biogas and digestate supply strategies. *Chem Eng J* 354, 363–369. <https://doi.org/10.1016/j.cej.2018.08.026>.
- Fuess, L.T., Braga, A.F.M., Eng, F., Gregoracci, G.B., Saia, F.T., Zaiat, M., et al., 2023. Solving the bottlenecks of sugarcane vinasse biodigestion: impacts of temperature and substrate exchange on sulfate removal during dark fermentation. *Chem Eng J* 455 (Part 2). <https://doi.org/10.1016/j.cej.2022.140965>.
- Fuess, L.T., Braga, A.F., Zaiat, M., Lens, P.N., 2023. Solving the seasonality issue in sugarcane biorefineries: High-rate year-round methane production from fermented

- sulfate-free vinasse and molasses. *Chem Eng J* 478, 147432. <https://doi.org/10.1016/j.cej.2023.147432>.
- [29] Fuess, L.T., García, M.L., 2014. Implications of stillage land disposal: a critical review on the impacts of fertigation. *J Environ Manag* 145, 210–229. <https://doi.org/10.1016/j.jenvman.2014.07.003>.
- [30] Fuess, L.T., García, M.L., Zaiat, M., 2018. Seasonal characterization of sugarcane vinasse: assessing environmental impacts from fertigation and the bioenergy recovery potential through biodigestion. *Sci Total Environ* 634, 29–40. <https://doi.org/10.1016/j.scitotenv.2018.03.326>.
- [31] Fuess, L.T., Kiyuna, L.S.M., Júnior, A.D.N.F., Persinoti, G.F., Squina, F.M., García, M.L., et al., 2017. Thermophilic two-phase anaerobic digestion using an innovative fixed-bed reactor for enhanced organic matter removal and bioenergy recovery from sugarcane vinasse. *Appl Energy* 189, 480–491. <https://doi.org/10.1016/j.apenergy.2016.12.071>.
- [32] Fuess, L.T., Piffer, M.A., Zaiat, M., do Nascimento, C.A.O., 2022. Phase separation enhances bioenergy recovery in sugarcane vinasse biodigestion: absolute or relative truth? *Bioresour Technol Rep* 18, 101026. <https://doi.org/10.1016/j.biteb.2022.101026>.
- [33] González-Camejo, J., Aparicio, S., Jiménez-Benítez, A., Pachés, M., Ruano, M.V., Borrás, L., et al., 2020. Improving membrane photobioreactor performance by reducing light path: operating conditions and key performance indicators. *Water Res* 172, 115518. <https://doi.org/10.1016/j.watres.2020.115518>.
- [34] González-Sánchez, A., Posten, C., 2017. Fate of H₂S during the cultivation of *Chlorella* sp. Deployed for biogas upgrading. *J Environ Manag* 191, 252–257. <https://doi.org/10.1016/j.jenvman.2017.01.023>.
- [35] Hasnain, M., Zainab, R., Ali, F., Abideen, Z., Yong, J.W.H., El-Keblawy, A., et al., 2023. Utilization of microalgal-bacterial energy nexus improves CO₂ sequestration and remediation of wastewater pollutants for beneficial environmental services. *Ecotoxicol Environ Saf* 267, 115646. <https://doi.org/10.1016/j.ecoenv.2023.115646>.
- [36] Hoyos, E.G., Amo-Duodu, G., Kiral, U.G., Vargas-Estrada, L., Lebrero, R., Muñoz, R., 2024. Influence of carbon-coated zero-valent iron-based nanoparticle concentration on continuous photosynthetic biogas upgrading. *Fuel* 356, 129610. <https://doi.org/10.1016/j.fuel.2023.129610>.
- [37] Huang, Q., Jiang, F., Wang, L., Yang, C., 2017. Design of photobioreactors for mass cultivation of photosynthetic organisms. *Engineering* 3 (3), 318–329. <https://doi.org/10.1016/j.eng.2017.03.020>.
- [38] Ji, M.K., Abou-Shanab, R.A., Kim, S.H., Salama, E.S., Lee, S.H., Kabra, A.N., et al., 2013. Cultivation of microalgae species in tertiary municipal wastewater supplemented with CO₂ for nutrient removal and biomass production. *Ecol Eng* 58, 142–148. <https://doi.org/10.1016/j.ecoleng.2013.06.020>.
- [39] Kim, J.H., Rene, E.R., Park, H.S., 2008. Biological oxidation of hydrogen sulfide under steady and transient state conditions in an immobilized cell biofilter. *Bioresour Technol* 99 (3), 583–588. <https://doi.org/10.1016/j.biortech.2006.12.028>.
- [40] Kiyuna, L.S.M., Fuess, L.T., Zaiat, M., 2017. Unraveling the influence of the COD/sulfate ratio on organic matter removal and methane production from the biodigestion of sugarcane vinasse. *Bioresour Technol* 232, 103–112. <https://doi.org/10.1016/j.biortech.2017.02.028>.
- [41] Lebrero, R., Toledo-Cervantes, A., Muñoz, R., Del Nery, V., Foresti, E., 2016. Biogas upgrading from vinasse digesters: a comparison between an anoxic biotrickling filter and an algal-bacterial photobioreactor. *J Chem Technol Biotechnol* 91, 2488–2495. <https://doi.org/10.1002/jctb.4843>.
- [42] Lens, P., N.L., Kuenen, J.G., 1998. The biological sulfur cycle: novel opportunities for environmental biotechnology. *Water Sci Technol* 44 (8), 57–66. <https://doi.org/10.2166/wst.2001.0464>.
- [43] Li, X., Jiang, X., Zhou, Q., Jiang, W., 2016. Effect of S/N ratio on the removal of hydrogen sulfide from biogas in anoxic bioreactors. *Appl Biochem Biotechnol* 180 (5), 930–944. <https://doi.org/10.1007/s12010-016-2143-3>.
- [44] Lin, S., Mackey, H.R., Hao, T., Guo, G., Van Loosdrecht, M.C.M., Chen, G., 2018. Biological sulfur oxidation in wastewater treatment: a review of emerging opportunities. *Water Res* 143, 399–415. <https://doi.org/10.1016/j.watres.2018.06.051>.
- [45] Lourenco, K.S., Rossetto, R., Vitti, A.C., Montezano, Z.F., Soares, J.R., de Melo Sousa, R., et al., 2019. Strategies to mitigate the nitrous oxide emissions from nitrogen fertilizer applied with organic fertilizers in sugarcane. *Sci Total Environ* 650, 1476–1486. <https://doi.org/10.1016/j.biombioe.2025.107603>.
- [46] Malone Rubright, S.L., Pearce, L.L., Peterson, J., 2017. Environmental toxicology of hydrogen sulfide. *Nitric oxide Biol Chem* 71, 1–13. <https://doi.org/10.1016/j.niox.2017.09.011>.
- [47] Marazzi, F., Bellucci, M., Fornaroli, R., Bani, A., Ficari, E., Mezzanotte, V., 2020. Lab-scale testing of operation parameters for algae-based treatment of piggy wastewater. *J Chem Technol Biotechnol* 95 (4), 967–974. <https://doi.org/10.1002/jctb.5972>.
- [48] Marín, D., Carmona-Martínez, A.A., Blanco, S., Lebrero, R., Muñoz, R., 2021. Innovative operational strategies in photosynthetic biogas upgrading in an outdoors pilot scale algal-bacterial photobioreactor. *Chemosphere* 264, 128470. <https://doi.org/10.1016/j.chemosphere.2020.128470>.
- [49] Marín, D., Ortíz, A., Díez-Montero, R., Uggetti, E., García, J., Lebrero, R., et al., 2019. Influence of liquid-to-biogas ratio and alkalinity on the biogas upgrading performance in a demo scale algal-bacterial photobioreactor. *Bioresour Technol* 280, 112–117. <https://doi.org/10.1016/j.biortech.2019.02.029>.
- [50] Marín, D., Posadas, E., Cano, P., Pérez, V., Blanco, S., Lebrero, R., et al., 2018. Seasonal variation of biogas upgrading coupled with digestate treatment in an outdoors pilot scale algal-bacterial photobioreactor. *Bioresour Technol* 263, 58–66. <https://doi.org/10.1016/j.biortech.2018.04.117>.
- [51] Marín, D.F., Posadas Olmos, E., Cano, P., Pérez Martínez, V., Lebrero Fernández, R., Muñoz Torre, R., 2018. Influence of the seasonal variation of environmental conditions on biogas upgrading in an outdoors pilot scale high-rate algal pond. *Bioresour Technol* 255, 354–358. <https://doi.org/10.1016/j.biortech.2018.01.136>.
- [52] Marques, S.S.I., Nascimento, I.A., Almeida, P.F., Chinalla, F.A., 2013. Growth of *Chlorella vulgaris* on sugarcane vinasse: the effect of anaerobic digestion pretreatment. *Appl Biochem Biotechnol* 171, 1933–1943. <https://doi.org/10.1007/s12010-013-0481-y>.
- [53] Mello, B.S., Sarti, A., Muñoz, R., 2025. Long-term effects of liquid nanoparticles on algal growth and photosynthetic biogas upgrading. *Renew Energy*, 123467. <https://doi.org/10.1016/j.renene.2025.123467>.
- [54] Méndez, L., García, D., Perez, E., Blanco, S., Muñoz, R., 2022. Photosynthetic upgrading of biogas from anaerobic digestion of mixed sludge in an outdoors algal-bacterial photobioreactor. *J Water Process Eng* 48, 102891. <https://doi.org/10.1016/j.jwpe.2022.102891>.
- [55] Montebello, A.M., Bezerra, T., Rovira, R., Rago, L., Lafuente, J., Gamisans, X., et al., 2013. Operational aspects, pH transition and microbial shifts of a H₂S desulfurizing biotrickling filter with random packing material. *Chemosphere* 93 (11), 2675–2682. <https://doi.org/10.1016/j.chemosphere.2013.08>.
- [56] Montebello, A.M., Baeza, M., Lafuente, J., Gabriel, D. Monitoring and performance of a desulfurizing biotrickling filter with an integrated continuous gas/liquid flow analyzer. *Chemical Engineering Journal*, 165, 2, 500–507, 2010. doi.org/10.1016/j.cej.2010.09.053.
- [57] Muñoz, R., Guieysse, B., 2006. Algal-bacterial processes for the treatment of hazardous contaminants: a review. *Water Res* 40 (15), 2799–2815. <https://doi.org/10.1016/j.watres.2006.06.011>.
- [58] Muñoz, R., Meier, L., Diaz, I., Jeison, D., 2015. A critical review on the state-of-the-art of physical/chemical and biological technologies for an integral biogas upgrading. *Rev. Environ. Sci. Biotechnol.* 14, 727–759. <https://doi.org/10.1007/s11157-015-9379-1>.
- [59] Nhut, H.H., Thanh, V.L.T., Le, L.T., 2020. Removal of H₂S in biogas using biotrickling filter: recent development. *Process Saf Environ Prot* 144, 297–309. <https://doi.org/10.1016/j.psep.2020.07.011>.
- [60] Piffer, M.A., Zaiat, M., Nascimento, C.A.O., Fuess, L.T., 2021. Dynamics of sulfate reduction in the thermophilic dark fermentation of sugarcane vinasse: a biohydrogen-independent approach targeting enhanced bioenergy production. *J Environ Chem Eng* 9 (5), 105956. <https://doi.org/10.1016/j.jece.2021.105956>.
- [61] Posadas, E., Marín, D., Blanco, S., Lebrero, R., Muñoz, R., 2017. Simultaneous biogas upgrading and centrate treatment in an outdoors pilot scale high-rate algal pond. *Bioresour Technol* 232, 133–141. <https://doi.org/10.1016/j.biortech.2017.01.071>.
- [62] Posadas, E., Muñoz, A., García-González, M.C., Muñoz, R., García-Encina, P.A., 2014. A case study of a pilot high-rate algal pond for the treatment of fish farm and domestic wastewaters. *J Chem Technol Biotechnol* 90, 1094–1101. <https://doi.org/10.1002/jctb.4417>.
- [63] Posadas, E., Serejo, M.L., Blanco, S., Pérez, R., García-Encina, P.A., Muñoz, R., 2015. Minimization of biomethane oxygen concentration during biogas upgrading in algal-bacterial photobioreactors. *Algal Res* 12, 221–229. <https://doi.org/10.1016/j.algal.2015.09.002>.
- [64] Posadas, E., Szpak, D., Lombó, F., Domínguez, A., Díaz, I., Blanco, S., et al., 2016. Feasibility study of biogas upgrading coupled with nutrient removal from anaerobic effluents using microalgae-based processes. *J Appl Phycol* 28, 2147–2157. <https://doi.org/10.1007/s10811-015-0758-3>.
- [65] Price, G.D., Woodger, F.J., Badger, M.R., Howitt, S.M., Tucker, L., 2004. Identification of a SulP-type bicarbonate transporter in marine Cyanobacteria. *Proc Natl Acad Sci USA* 101 (52), 18228–18233. <https://doi.org/10.1073/pnas.0405211101>.
- [66] Pudi, A., Rezaei, M., Signorini, V., Andersson, M.P., Baschetti, M.G., Mansouri, S.S., 2022. Hydrogen sulfide capture and removal technologies: a comprehensive review of recent developments and emerging trends. *Sep Purif Technol* 298, 121448. <https://doi.org/10.1016/j.seppur.2022.121448>.
- [67] Raj, A., Ibrahim, S., Jagannath, A., 2020. Combustion kinetics of H₂S and other sulfur species with relevance to industrial processes. *Prog Energy Combust Sci* 80, 100848. <https://doi.org/10.1016/j.pecs.2020.100848>.
- [68] Rocher-Rivas, R., González-Sánchez, A., Ulloa-Mercado, G., Muñoz, R., Quijano, G., 2022. Biogas desulfurization and calorific value enhancement in compact H₂S/CO₂ absorption units coupled to a photobioreactor. *J Environ Chem Eng* 10 (5), 108336. <https://doi.org/10.1016/j.jece.2022.108336>.
- [69] Rodero, M., Carvajal, A., Castro, V., Navia, D., De Prada, C., Lebrero, R., et al., 2019. Development of a control strategy to cope with biogas flowrate variations during photosynthetic biogas upgrading. *Biomass Bioenergy* 131, 105414. <https://doi.org/10.1016/j.biombioe.2019.105414>.
- [70] Rodero, M., Posadas, E., Toledo-Cervantes, A., Lebrero, R., Muñoz, R., 2018. Influence of alkalinity and temperature on photosynthetic biogas upgrading efficiency in high-rate algal ponds. *Algal Res* 33, 284–290. <https://doi.org/10.1016/j.algal.2018.06.001>.
- [71] Rodero, M., Severi, C.A., Rocher-Rivas, R., Quijano, G., Muñoz, R., 2020. Long-term influence of high alkalinity on the performance of photosynthetic biogas upgrading. *Fuel* 281, 118804. <https://doi.org/10.1016/j.fuel.2020.118804>.
- [72] Rodríguez, G., Dorado, A.D., Fortuny, M., Gabriel, D., Gamisans, X., 2014. Biotrickling filters for biogas sweetening: oxygen transfer improvement for a reliable operation. *Process Saf Environ Prot* 92 (3), 261–268. <https://doi.org/10.1016/j.psep.2013.02.002>.
- [73] Rogeri, R.C., Fuess, L.T., De Araujo, M.N., Eng, F., Borges, A.V., Damianovic, M.H. R.Z., et al., 2024. Methane production from sugarcane vinasse: the alkalizing

- potential of fermentative-sulfidogenic processes in two-stage anaerobic digestion. *Energy Nexus* 14, 100303. <https://doi.org/10.1016/j.nexus.2024.100303>.
- [74] Rogeri, R.C., Fuess, L.T., Eng, F., Borges, A.V., Araujo, M.N., Damianovic, M.H.R. Z., et al., 2023. Strategies to control pH in the dark fermentation of sugarcane vinasse: impacts on sulfate reduction, biohydrogen production and metabolite distribution. *J Environ Manag* 325 (Part B). <https://doi.org/10.1016/j.jenvman.2022.116495>.
- [75] San-Valero, P., Peña-Roja, J.M., Álvarez-Hornos, F.J., Buitrón, G., Gabaldón, C., Quijano, G., 2019. Fully aerobic bioscrubber for the desulfurization of H₂S-rich biogas. *Fuel* 241, 884–891. <https://doi.org/10.1016/j.fuel.2018.12.098>.
- [76] Scarcelli, P.G., Ruas, G., Lopez-Serna, R., Serejo, M.L., Blanco, S., Boncz, M.A., et al., 2021. Integration of algae-based sewage treatment with anaerobic digestion of the bacterial-algal biomass and biogas upgrading. *Bioresour Technol* 340, 125552. <https://doi.org/10.1016/j.biortech.2021.125552>.
- [77] Sepúlveda-Munoz, C.A., Hontiyuelo, G., Blanco, S., Torres-Franco, A.F., Munoz, R., 2022. Photosynthetic treatment of piggery wastewater in sequential purple phototrophic bacteria and microalgae-bacteria photobioreactors. *J Water Process Eng* 47, 102825. <https://doi.org/10.1016/j.jwpe.2022.102825>.
- [78] Serejo, M.L., Ruas, G., Braga, G.B., Paulo, P.L., Boncz, M.A., 2021. *Chlorella vulgaris* growth on anaerobically digested sugarcane vinasse: influence of turbidity. *da Acad Bras De Ciências* 93 (1), e20190084. <https://doi.org/10.1590/0001-3765202120190084>.
- [79] Severi, C.A., Pascual, C., Perez, V., Muñoz, R., Lebrero, R., 2025. Pilot-Scale biogas desulfurization through anoxic biofiltration. *J Hazard Mater* 485, 136830. <https://doi.org/10.1016/j.jhazmat.2024.136830>.
- [80] Sournia, A. *Phytoplankton Manual*. Museum National d' Historie Naturelle, Paris, United Nations Educational, Scientific and Cultural Organization (Unesco); 1978.
- [81] Struk, M., Sepúlveda-Munoz, C.A., Kushkevych, I., Muñoz, 2023. Photoautotrophic removal of hydrogen sulfide from biogas using purple and Green sulfur bacteria. *J Hazard Mater* 443 (Part B), 130337. <https://doi.org/10.1016/j.jhazmat.2022.130337>.
- [82] Takahashi, H., Kopriva, S., Giordano, M., Saito, K., Hell, R., 2011. Sulfur assimilation in photosynthetic organisms: molecular functions and regulations of transporters and assimilatory enzymes. *Annu Rev Plant Biol* 62 (1), 157–184. <https://doi.org/10.1146/annurev-arplant-042110-103921>.
- [83] Toledo-Cervantes, A., Madrid-Chirinos, C., Cantera, S., Lebrero, R., Muñoz, R., 2017. Influence of the gas-liquid flow configuration in the absorption column on photosynthetic biogas upgrading in algal-bacterial photobioreactors. *Bioresour Technol* 225, 336–342. <https://doi.org/10.1016/j.biortech.2016.11.087>.
- [84] Toledo-Cervantes, A., Morales, T., González, A., Muñoz, R., Lebrero, R., 2018. Long-term photosynthetic CO₂ removal from biogas and flue-gas: exploring the potential of closed photobioreactors for high-value biomass production. *Sci Total Environ* 640, 1272–1278. <https://doi.org/10.1016/j.scitotenv.2018.05.270>.
- [85] Toledo-Cervantes, A., Serejo, M.L., Blanco, S., Pérez, R., Lebrero, R., Muñoz, R., 2016. Photosynthetic biogas upgrading to bio-methane: boosting nutrient recovery via biomass productivity control. *Algal Res* 17, 46–52. <https://doi.org/10.1016/j.algal.2016.04.017>.
- [86] Toro-Huertas, E.I., Franco-Morgado, M., de los Cobos Vasconcelos, D., González-Sánchez, A., 2019. Photorespiration in an outdoor alkaline open-photobioreactor used for biogas upgrading. *Sci Total Environ* 667, 613–621. <https://doi.org/10.1016/j.scitotenv.2019.02.374>.
- [87] Vikromvarasiri, N., Champreda, V., Boonyawanich, S., Pisutpaisal, N., 2017. Hydrogen sulfide removal from biogas by biotrickling filter inoculated with *halothiobacillus neapolitanus*. *Int J Hydrog Energy* 42 (29), 18425–18433. <https://doi.org/10.1016/j.ijhydene.2017.05.020>.
- [88] Wang, N., Bai, S., Zhang, Y.N., Xu, D., Zhang, Q., Wang, M., et al., 2025. Sulfur autotrophic denitrification as a sustainable nitrogen removal technology to achieve carbon neutrality: recent advances and optimization strategies. *J Water Process Eng* 70, 107154. <https://doi.org/10.1016/j.jwpe.2025.107154>.
- [89] Wang, X., Bao, K., Cao, W., Zhao, Y., Hu, C.W., 2017. Screening of microalgae for integral biogas slurry nutrient removal and biogas upgrading by different microalgae cultivation technology. *Sci Rep* 7 (1), 5426. <https://doi.org/10.1038/s41598-017-05841-9>.
- [90] Wasim, M., Djukic, M.B., 2022. External corrosion of oil and gas pipelines: a review of failure mechanisms and predictive prevention. *J Nat Gas Sci Eng* 100, 104467. <https://doi.org/10.1016/j.jngse.2022.104467>.
- [91] Xu, P., Fan, H., Leng, L., Fan, L., Liu, S., Chen, P., et al., 2020. Feasibility of microbially induced carbonate precipitation through a *Chlorella-sporosarcina* co-culture system. *Algal Res* 47, 101831. <https://doi.org/10.1016/j.algal.2020.101831>.
- [92] Zhang, B., Wang, Y., Zhu, H., Huang, S., Zhang, J., Wu, X., et al., 2022. Evaluation of H₂S gas removal by a biotrickling filter: effect of oxygen dose on the performance and microbial communities. *Process Saf Environ Prot* 166, 30–40. <https://doi.org/10.1016/j.psep.2022.07.054>.